

COMMUNICATION

Fluorescence-detected magnetic field effects on radical pair reactions from femtolitre volumes

Published version:

DOI: [10.1039/C5CC01099C](https://doi.org/10.1039/C5CC01099C)

Chem. Commun., 51, 8023–8026, (2015)

C. A. Dodson,^{‡ae} C. J. Wedge,^{‡bf} M. Murakami,^c K. Maeda,^{cdg}, M. I. Wallace^a and P. J. Hore^{*b}

Received 5th February 2015,

Accepted 25th March 2015

DOI: [10.1039/C5CC01099C](https://doi.org/10.1039/C5CC01099C)www.rsc.org/

We show that the effects of applied magnetic fields on radical pair reactions can be sensitively measured from sample volumes as low as ~100 femtolitres using total internal reflection fluorescence microscopy. Development of a fluorescence-based microscope method is likely to be a key step in further miniaturisation that will allow detection of magnetic field effects on single molecules.

Flavins — tricyclic aza-aromatic compounds — occur widely in Nature and perform a variety of biological functions, many of which involve electron transfer.¹ Attention has recently focussed on the flavoprotein cryptochrome which has been proposed as the primary sensory molecule by which migratory birds detect the direction of the Earth's magnetic field.^{2–5} Blue-light excitation of the flavin adenine dinucleotide (FAD) chromophore in cryptochrome is thought to trigger intra-protein electron transfers along a triad of tryptophan (Trp) residues to give a stabilised, charge-separated FAD-Trp radical pair.^{6–9} Transient absorption studies¹⁰ have shown that coherent interconversion of the electronic singlet and triplet states of the radical pair gives rise to long lived states of the protein whose quantum yields can be modified by applied magnetic fields via the well-established radical pair mechanism.^{11, 12}

Studies of the magnetic sensitivity of cryptochromes are currently constrained by the relatively high protein concentrations and large sample volumes required for absorption-based spectroscopy and by the photo-degradation caused by the intense laser pulses often needed for such measurements.^{13, 14} Cryptochromes — in particular the vertebrate proteins — are difficult to express recombinantly in large quantities and tend to aggregate in concentrated solution. Further *in vitro* studies of their magnetic responses will require a detection

method compatible with much smaller quantities of protein, the obvious choice being fluorescence.

Fluorescence has been used extensively to monitor magnetic field effects (MFEs) on the photochemistry of small organic radicals. In appropriate, usually non-aqueous, solvents singlet but not triplet radical pairs can often recombine to form an exciplex whose fluorescence provides a convenient and sensitive probe of the magnetic response.^{15–18} Effective though such an approach has proved, it is manifestly inapplicable when the radical pair cannot recombine to form a luminescent state. Many radical pairs, including flavin-Trp, do not form excited molecular complexes and cryptochromes have no other electronically excited states that can be populated from the FAD-Trp radical pair.

However, flavins do have fluorescent excited states that can be exploited as MFE probes. For cyclic photochemical reactions under conditions of continuous illumination, the fluorescence intensity reflects the steady state concentration of ground state flavin, which in turn depends on the concentrations of long-lived radical intermediates in the photocycle. If all other species are short lived and thus present in low concentrations, any increase in the steady state concentration of long lived radicals must be balanced by a corresponding decrease in the concentration of the flavin ground state and therefore in the fluorescence. Prompt emission arising from photo-excitation of the ground state is thus an alternative means of studying the effects of applied magnetic fields.

We report here a new method for studying MFEs on flavin photo-reactions using total internal reflection fluorescence (TIRF) microscopy.¹⁹ The advantages include the ability to detect signal from a small area (~30 µm × 30 µm) of a thin layer of solution (~100 nm) and the opportunity to use much smaller quantities of precious samples. Moving to microscopy-based fluorescence

measurements will also be crucial for attempts to measure MFEs on single molecules. To determine whether cryptochromes display the properties expected of biological compass sensors, it will be necessary to characterise their directional responses to weak external magnetic fields. Such an advance is likely to exploit measurements on surface-immobilized single molecules, avoiding the need for bulk alignment of a protein sample.

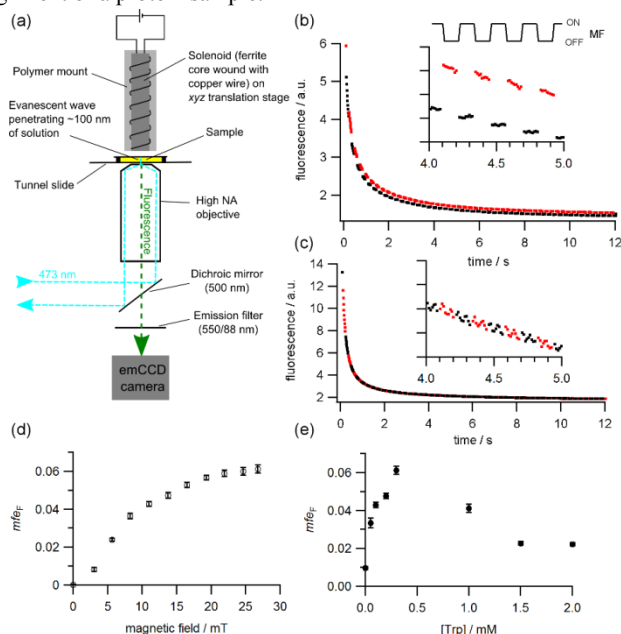


Fig. 1 Fluorescence detection of MFEs. (a) Schematic diagram of the experiment. (b) Fluorescence signals from 1 μM FAD + 300 μM Trp solutions. Red/black: data measured in absence/presence of a 26.8 mT magnetic field. A portion of the signal is shown inset. (c) As (b) but 1 μM FMN without Trp. (d) Fractional MFE (1 μM FAD + 300 μM Trp) as a function of B_0 . (e) Fractional MFE (1 μM FAD) as a function of Trp concentration for $B_0 = 26.8$ mT.

In this preliminary communication, we report TIRF measurements of MFEs on both flavin-adenine and flavin-Trp radical pairs formed, respectively, by intra- and intermolecular electron transfer reactions of photo-excited triplet FAD.^{20, 21}

The fluorescence of FAD-Trp solutions at low pH, generated by a 473 nm continuous-wave laser, was monitored by TIRF microscopy (Fig. 1a) in the presence of a square-wave modulated static magnetic field. Fluorescence was detected from a ~ 100 fL volume of solution (see Materials and Methods, ESI† for details). The switched magnetic field produced a clear stepwise modulation of the fluorescence (Fig. 1b) with a significant reduction in the emission at the beginning, and a comparable increase at the end, of each field pulse. This is as expected for a triplet-born radical pair: the Zeeman interaction of the electron spins in the radical pair isolates the T_{+1} and T_{-1} triplet states from the T_0 triplet and S (singlet) states and so inhibits the formation of singlet radical pairs and therefore, also, the return to the ground state.²⁰ Similar fluorescence-detected MFEs were observed for FAD in the absence of Trp, but not for controls containing flavin mononucleotide (FMN), which does not contain the adenine electron donor (Fig. 1c), or fluorescein or Alexa Fluor® 488 which would not be expected to show a MFE (Fig. S1, ESI†).

Magnetic field effects were quantified by means of the parameter $mfe_F = [F(0) - F(B_0)]/F(0)$ (see ESI† for details). $F(B_0)$ and $F(0)$ are

the fluorescence intensities during the periods when the magnetic field is, respectively, present (at strength B_0) and absent (black and red sections of Fig. 1b). This fractional MFE increased with B_0 , tending to level out, as expected,²⁰ when the applied field exceeded the effective hyperfine interaction of the radical pair (Fig. 1d). As the Trp concentration was increased in the range 0–300 μM , mfe_F rose from 1% to 6% and fell back to 2% at ~ 2 mM (Fig. 1e).

The field-induced changes in FAD fluorescence were observed on a background of steadily decreasing overall fluorescence (Fig. 1b). This decay was also observed for FMN (Fig. 1c) and fluorescein (Fig. S1, ESI†) and is attributed, at least in part, to photobleaching.

To validate our TIRF approach and to gain more mechanistic information, we studied the same FAD-Trp solutions by transient absorption in order to distinguish the various states of the reactants and their kinetics. The neutral, protonated flavin radical, FADH^\bullet , is characterised by a broad absorption in the range 500–600 nm overlapping that of the Trp cation radical ($\text{Trp}^{\bullet+}$); the absorption of the excited triplet flavin, ^3FAD , extends to longer wavelengths, 500–700 nm (Fig. S2, ESI†). FAD itself absorbs at wavelengths below 500 nm and Trp is transparent at wavelengths above ~ 300 nm.²²

The transient absorption signals of FAD-Trp solutions monitored at 580 nm (where $\text{Trp}^{\bullet+}$, FADH^\bullet and ^3FAD have comparable extinctions) showed a biphasic decay with the lifetime of the slow component increasing significantly in the presence of Trp (Fig. 2a). The time-dependent absorption at 650 nm, where ^3FAD is the dominant contributor, was also biphasic (Fig. 2b). In the absence of Trp, the signals at the two wavelengths (red traces in Figs 2a & b) are very similar and differ only in amplitude, reflecting the wavelength-dependence of the extinction coefficients. This indicates that the decay of ^3FAD in the absence of Trp also dominates the 580 nm signal in agreement with Murakami et al.²¹ In the presence of Trp, the absorbance at 650 nm was rapidly quenched (Fig. 2b) and the amplitude of the slow phase observed at 580 nm increased (Fig. 2a). We therefore assign the slow decay at 580 nm to long lived FADH^\bullet and/or $\text{Trp}^{\bullet+}$ radicals formed by $^3\text{FAD} + \text{Trp}$ reaction.

MFE time-profiles were calculated as the change in the transient absorbance produced by an applied magnetic field: $\Delta\Delta A = \Delta A(B_0) - \Delta A(0)$. $\Delta\Delta A_{540-600}$ data for $B_0 = 200$ mT, averaged over the wavelength range 540–600 nm, showed a fast component at Trp concentrations below ~ 0.1 mM and a much slower component at higher concentrations (Fig. 2c and Fig. S3, ESI†). At longer wavelengths (630–710 nm) the fast component dominated and its amplitude and lifetime decreased markedly with increasing Trp concentration (Fig. 2d). The MFE detected by absorption is positive, i.e. $\Delta A(B_0) > \Delta A(0)$, consistent with the negative effect observed by fluorescence, $F(B_0) < F(0)$.

$\Delta\Delta A_{630-710}$ is dominated by magnetically sensitive changes in the population of ^3FAD while $\Delta\Delta A_{540-600}$ monitors FADH^\bullet and $\text{Trp}^{\bullet+}$ as well as ^3FAD . In the absence of Trp (red traces, Fig. 2c and d), ^3FAD is, once again, the major contributor to the signals at both wavelengths. The changes brought about by the addition of Trp are attributed to the reaction of ^3FAD with Trp to form long lived FADH^\bullet and $\text{Trp}^{\bullet+}$ radicals (slow components in Fig. 2c and Fig. S3, ESI†).

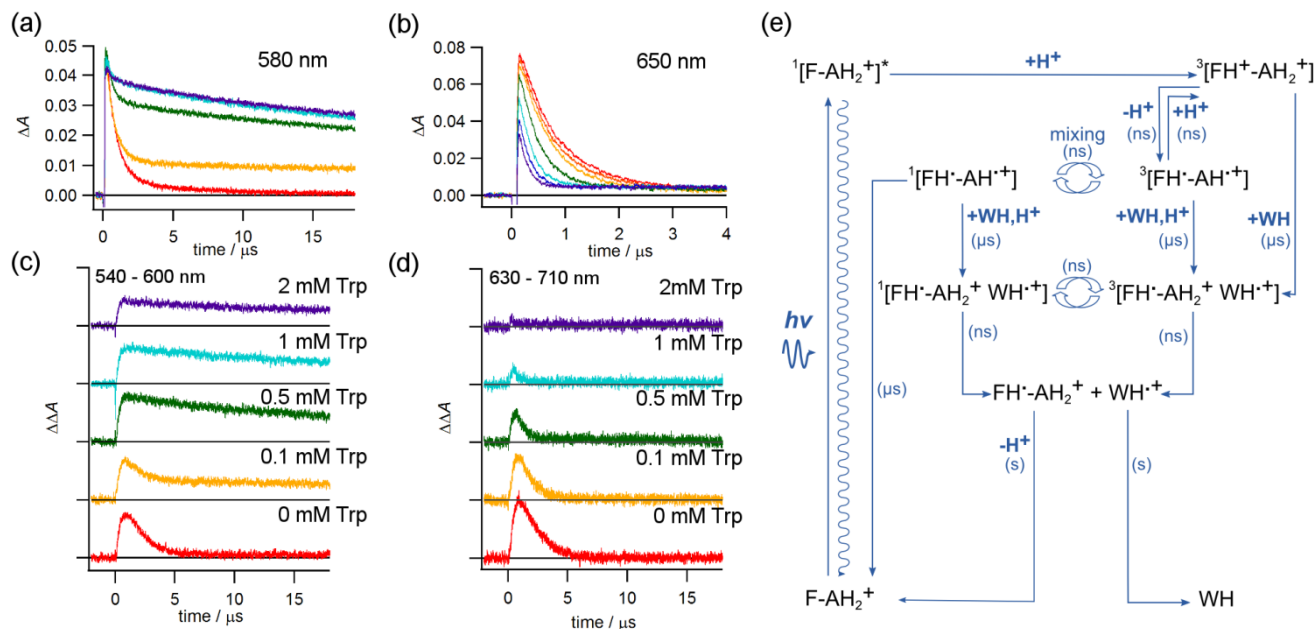


Fig. 2 Transient absorption detection of MFEs. Time-dependence of the absorbance change at (a) 580 nm and (b) 650 nm. The colour code for the Trp concentrations in (a) and (b) is the same as in (c) and (d). MFE time-profiles averaged over the wavelength ranges (c) 540–600 nm and (d) 630–710 nm. (e) FAD photocycle including the FAD + Trp reaction. FAD is shown as $F-AH_2$ with the flavin (isoalloxazine) and adenine groups denoted F and A. Trp is denoted W.

The transient absorption measurements summarized in Fig. 2a-d enable us to extend the previously published FAD photocycle²¹ to include the FAD + Trp reaction (Fig. 2e). Blue-light illumination of ground state FAD produces the excited singlet state which either fluoresces or intersystem crosses to 3FAD . Electron transfer from the adenine to the isoalloxazine of FAD in 3FAD forms a geminate triplet flavin-adenine radical pair which undergoes magnetically sensitive triplet \leftrightarrow singlet interconversion. The rapid reversibility of the electron transfer step is indicated by the MFE on 3FAD as observed previously.²¹

Reverse electron transfer in the singlet state of the flavin-adenine radical pair provides a return route to ground state FAD. Additionally, 3FAD can be quenched by Trp to form an intermolecular radical pair whose constituents ($FADH^\bullet$ and $Trp^{\bullet+}$) either undergo reverse electron transfer or diffuse apart to form the long lived free radicals that are responsible for the slow transient absorption components in Figs 2a and c. Due to the fast interconversion between 3FAD and the flavin-adenine radical pair, we cannot exclude the possibility that Trp reacts with the pre-existing intramolecular radical pair as well as with the triplet flavin.

As argued above, for a photocycle of the type shown in Fig. 2e, any field-induced increase in the steady state concentration of the long lived radicals is matched by a corresponding decrease in the concentration of the ground state molecules. This point can be seen clearly by comparing Figs 3a and c which show, respectively, $\Delta A(B_0) - \Delta A(0)$ and $F(0) - F(B_0)$. Both absorption- and fluorescence-detected MFEs show the same trend with increasing Trp concentration. Similarly, the increase in the yield of long lived radicals observed by transient absorption (Fig. 3b) is complemented by a decrease in the ground state concentration observed by fluorescence (Fig. 3d).

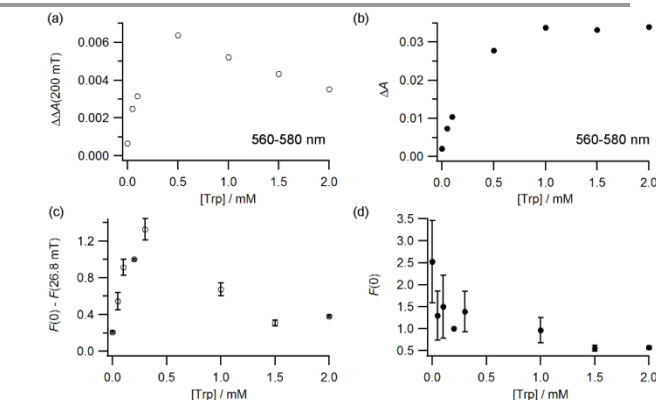


Fig. 3 Comparison of absorption- and fluorescence-detected MFEs. (a) Transient absorption difference signal, $\Delta A = \Delta A(200 \text{ mT}) - \Delta A(0)$. (b) Transient absorption signal in the absence of a magnetic field, $\Delta A(0)$. (c) Fluorescence difference signal $F(0) - F(26.8 \text{ mT})$. (d) Initial fluorescence intensity in the absence of a magnetic field. The data in panels (a) and (b) are averages over the wavelength range 560–580 nm and the time period 5–10 μ s. The data in panels (c) and (d) have been normalised to the measurement at 200 μ M Trp and error bars show SEM. The FAD concentrations were 0.2 mM (absorbance) and 1 μ M (fluorescence).

We have demonstrated for the first time that MFEs can be measured by TIRF microscopy and that flavin fluorescence probes the same magnetically-sensitive reaction steps as optical absorption of the transient radical intermediates. Fluorescence measurements are highly sensitive and thus suitable for much lower concentrations than absorption-based techniques, making them attractive for samples that are prone to concentration-dependent aggregation. By using an inverted microscope with a high numerical aperture objective and TIR illumination we have reduced the volume probed to $\sim 100 \text{ fL}$. Together, these developments reduce the total sample requirement by several orders of magnitude, opening the possibility of measuring MFEs on samples for which low yields or concentrations previously

made measurements impractical. Despite the low quantum yield of FAD fluorescence in cryptochromes (due to rapid electron transfer from the Trp triad), we believe it will be possible to study MFEs on the intra-protein FAD-Trp radical pairs. The miniaturisation afforded by fluorescence microscopy is also an important step on the journey towards the goal of magnetic field effect measurements on single molecules.

Like previous TIRF measurements on FAD²³, our method already possesses single-molecule sensitivity. However, further improvements will be needed for single-molecule MFE detection: either to resolve time-dependent switching between states, or to increase the precision in measurement of the mean photon emission rate during the photocycle. These advances could be achieved either by improvements in the time-resolution of the experiment, or modification of the photocycle kinetics.

We are grateful to Neville Baker, Howard Lambourne and Les Hill for technical assistance. This work was supported by the Defence Advanced Research Projects Agency (QuBE: N66001-10-1-4061), the European Research Council (under the European Union's 7th Framework Programme, FP7/2007-2013/ERC grant agreement no. 340451), the Air Force Office of Scientific Research (Air Force Materiel Command, USAF award no. FA9550-14-1-0095), EPSRC, and the EMF Biological Research Trust. KM is indebted to Prof. Tatsuo Arai for permission to use equipment in his laboratory at University of Tsukuba. The writing of this paper was assisted by an Imperial College Junior Research Fellowship to CD.

Notes and references

^a Department of Chemistry, University of Oxford, Chemistry Research Laboratory, 12 Mansfield Road, Oxford OX1 3TA, UK.

^b Department of Chemistry, University of Oxford, Physical and Theoretical Chemistry Laboratory, South Parks Road, Oxford OX1 3QZ, UK. E-mail: peter.hore@chem.ox.ac.uk

^c Department of Chemistry, University of Tsukuba, 1-1-1 Tenno-dai, Tsukuba City, Ibaraki Pref, 305-8571, Japan.

^d Centre for Advanced Electron Spin Resonance, Department of Chemistry, University of Oxford, Oxford OX1 3QR, UK.

^e Current address: Molecular Medicine, National Heart & Lung Institute, Imperial College London, SAF Building, London SW7 2AZ, UK.

^f Current address: Department of Physics, University of Warwick, Gibbet Hill Road, Coventry CV4 7AL, UK.

^g Current address: Department of Chemistry, Graduate School of Science and Engineering, Saitama University, 255 Shimo-Okubo, Sakura-ku, Saitama City, Saitama 338-8570, Japan.

‡ These authors contributed equally to this work.

† Electronic Supplementary Information (ESI) available: Materials and methods; Supplementary figures. See DOI: 10.1039/C5CC01099C/

1. I. Chaves, R. Pokorny, M. Byrdin, N. Hoang, T. Ritz, K. Brettel, L. O. Essen, G. T. J. van der Horst, A. Batschauer and M. Ahmad, *Annu. Rev. Plant Biol.*, 2011, **62**, 335-364.
2. T. Ritz, S. Adem and K. Schulten, *Biophys. J.*, 2000, **78**, 707-718.
3. C. T. Rodgers and P. J. Hore, *Proc. Natl. Acad. Sci. USA*, 2009, **106**, 353-360.
4. H. Mouritsen and P. J. Hore, *Curr. Opin. Neurobiol.*, 2012, **22**, 343-352.
5. C. A. Dodson, P. J. Hore and M. I. Wallace, *Trends Biochem. Sci.*, 2013, **38**, 435-446.
6. Y. M. Gindt, E. Vollenbroek, K. Westphal, H. Sackett, A. Sancar and G. T. Babcock, *Biochemistry*, 1999, **38**, 3857-3866.
7. B. Giovani, M. Byrdin, M. Ahmad and K. Brettel, *Nature Struct. Biol.*, 2003, **10**, 489-490.
8. A. Zeugner, M. Byrdin, J.-P. Bouly, N. Bakrim, B. Giovani, K. Brettel and M. Ahmad, *J. Biol. Chem.*, 2005, **280**, 19437-19440.
9. T. Biskup, E. Schleicher, A. Okafuji, G. Link, K. Hitomi, E. D. Getzoff and S. Weber, *Angew. Chem. Internat. Ed.*, 2009, **48**, 404-407.
10. K. Maeda, A. J. Robinson, K. B. Henbest, H. J. Hogben, T. Biskup, M. Ahmad, E. Schleicher, S. Weber, C. R. Timmel and P. J. Hore, *Proc. Natl. Acad. Sci. USA*, 2012, **109**, 4774-4779.
11. U. E. Steiner and T. Ulrich, *Chem. Rev.*, 1989, **89**, 51-147.
12. C. T. Rodgers, *Pure Appl. Chem.*, 2009, **81**, 19-43.
13. S. R. T. Neil, K. Maeda, K. B. Henbest, M. Goetz, R. Hemmens, C. R. Timmel and S. R. Mackenzie, *Mol. Phys.*, 2010, **108**, 993-1003.
14. K. Maeda, S. R. T. Neil, K. B. Henbest, S. Weber, E. Schleicher, P. J. Hore, S. R. Mackenzie and C. R. Timmel, *J. Amer. Chem. Soc.*, 2011, **133**, 17807-17815.
15. A. Weller, H. Staerk and R. Treichel, *Faraday Discuss.*, 1984, **78**, 271-278.
16. J. R. Woodward, C. R. Timmel, K. A. McLauchlan and P. J. Hore, *Phys. Rev. Lett.*, 2001, **87**, 077602.
17. G. Grampp, M. Justinek and S. Landgraf, *Mol. Phys.*, 2002, **100**, 1063-1070.
18. C. T. Rodgers, S. A. Norman, K. B. Henbest, C. R. Timmel and P. J. Hore, *J. Amer. Chem. Soc.*, 2007, **129**, 6746-6755.
19. D. Axelrod, T. P. Burghardt and N. L. Thompson, *Annu. Rev. Biophys. Biochem.*, 1984, **13**, 247-268.
20. E. W. Evans, C. A. Dodson, K. Maeda, T. Biskup, C. J. Wedge and C. R. Timmel, *Interface Focus*, 2013, **3**, 20130037.
21. M. Murakami, K. Maeda and T. Arai, *J. Phys. Chem. A*, 2005, **109**, 5793-5800.
22. M. Murakami, K. Maeda and T. Arai, *Chem. Phys. Lett.*, 2002, **362**, 123-129.
23. S. Solar, N. Getoff, P. S. Surdhar, D. A. Armstrong and A. Singh, *J. Phys. Chem.*, 1991, **95**, 3639-3643.

Fluorescence-detected magnetic field effects on radical pair reactions from femtolitre volumes

Charlotte A Dodson,^{1,5‡} C. J. Wedge,^{2,6‡} Masaaki Murakami,³ Kiminori Maeda,^{3,4,7} Mark I. Wallace,¹ and P. J. Hore^{2*}

‡ These authors contributed equally to this work

Email: peter.hore@chem.ox.ac.uk

¹Department of Chemistry, University of Oxford, Chemistry Research Laboratory, 12 Mansfield Road, Oxford OX1 3TA, UK

²Department of Chemistry, University of Oxford, Physical and Theoretical Chemistry Laboratory, South Parks Road, Oxford OX1 3QZ, UK

³Department of Chemistry, University of Tsukuba, 1-1-1 Tenno-dai, Tsukuba City, Ibaraki Pref, 305-8571, Japan

⁴Centre for Advanced Electron Spin Resonance, Department of Chemistry, University of Oxford, Oxford OX1 3QR, UK

⁵Current address: Molecular Medicine, National Heart & Lung Institute, Imperial College London, SAF Building, London SW7 2AZ, UK

⁶Current address: Department of Physics, University of Warwick, Gibbet Hill Road, Coventry CV4 7AL, UK

⁷Current address: Graduate School of Science and Engineering, Saitama University, 255 Shimo-Okubo, Sakura-ku, Saitama City, Saitama 338-8570, Japan

ELECTRONIC SUPPLEMENTARY INFORMATION

MATERIALS AND METHODS

Buffers

All measurements were made in citric acid-phosphate buffer (pH 2.3, 12 mM Na₂HPO₄ and 94 mM citric acid).

Microscopy

Solutions for measurement were placed in tunnel slides made from two perpendicular coverslips separated by a single layer of double sided tape (total sample volume ~30 μ L). The sample was excited through a 60 \times oil-immersion 1.45 N.A. TIRF objective on a Nikon TE-2000 inverted microscope using a 473 nm laser reflected by a dichroic filter (Semrock Brightline FF497-Di03), giving a <100 fL probe volume. Fluorescence transmitted through the dichroic filter was passed through an emission filter (Semrock Brightline 550/88) before fluorescence detection using an Andor iXon+ electron-multiplying CCD camera (emCCD, gain: 300) (Fig. 1a). Illumination intensity at the sample was 0.5 kW cm⁻² neglecting losses inside the microscope body and optics. Both camera firing and magnetic field switching were controlled by the output of a Quantum Composers 9520 pulse generator to ensure complete synchrony. The magnetic field was switched (on or off) every ten camera frames (102.4 ms) for the duration of recording (usually 1000 frames).

Calibration and determination of the rise time of the solenoid

Magnetic fields were generated using a solenoid wound around a 3 mm diameter ferrite core and fixed into a non-metallic mount using epoxy resin. A custom-built power supply drove the solenoid at an input frequency of up to 2 kHz and provided a maximum field strength at the tip of the

solenoid of over 27 mT. Calibration of the solenoid was performed using a gaussmeter based upon a Hall effect probe with 3 μ s rise time (Honeywell SS94A). The rise time of the magnetic field generated by the solenoid was found to be less than 70 μ s at the maximum achievable field strength.

The solenoid assembly was attached via a cantilever to a micrometer-resolution 3-axis translation stage mounted securely on the body of the inverted microscope. This arrangement allowed the solenoid position relative to the microscope objective to be reproducibly controlled, while an independent 2-axis translation stage was used to adjust the horizontal position of the sample. To centre the solenoid over the objective, coarse calibration was performed using bright-field microscopy images of the solenoid, followed by a magnetic field mapping experiment in which the MFE measured in a TIRF experiment was plotted against micrometer position to determine the centre field in the horizontal plane. All further MFE experiments were performed with the solenoid centred relative to the objective lens.

Fluorescence data processing

Camera frames (one every 10.24 ms) were separated according to the presence or absence of magnetic field, and the mean pixel intensity across each frame determined to give a single data point per frame. In order to ensure that data collected at the moment of field switching did not contain contributions from both field conditions, the data from such frames were discarded. To determine the magnetic field effect, eight values of mean pixel intensity within each sequence of ten points (representing measurements in the presence / absence of magnetic field, but excluding frames which may contain contributions from both conditions) were fit with a straight line. The line was extrapolated to the moment of field-switching and the step height between field on and off measurements determined by subtraction.

The value of $F(0) - F(B_0)$ varied over the first few data points collected, although it was constant at longer times (Fig. S4 a,b). This apparent time-dependence was also observed for FAD/Trp in the absence of magnetic fields (Fig. S4 c,d) and for FMN (which shows no magnetic field effect) in the presence of magnetic fields (Fig. S4 e,f). It is an artefact introduced by the initial steepness of the measured decay curves for the flavins, hence it was not observed for the photostable dye Alexa Fluor® 488 (Fig. S4 g,h). In order to enable as much of the data as possible to contribute to the final value, traces of mfe_F versus time were fit by an exponential decay plus a straight line and the y-intercept of the extrapolated straight line taken as the measured mfe_F value.

Transient absorption

Transient absorption spectra were observed using custom-built equipment. A flow system was used to transfer the sample into a quartz optical cell (optical path length 4 mm) where photochemical reactions were initiated by a laser pulse. The third harmonic ($\lambda = 355$ nm) of a Nd:YAG Laser (Spectra Physics GCR-3) was used as the excitation light source. The energy of the laser was adjusted to 15 mJ per pulse. The laser pulse repetition rate was 5 Hz. A 500 W Xe lamp (Ushio UXL-500SX) was used as a probe light source. The transient absorption signal was detected by a photomultiplier tube (Hamamatsu R928) preceded by a monochromator (Jasco CT-25) and was recorded by a digital oscilloscope (LeCroy LT-344).

SUPPLEMENTARY FIGURES

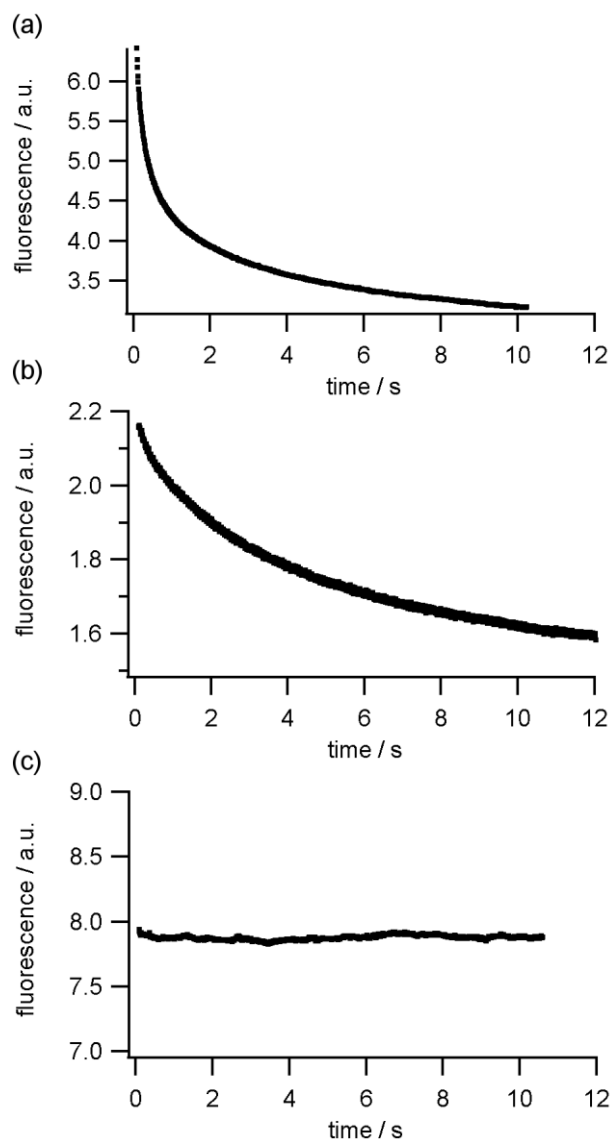


Fig. S1: Fluorescence decay curves for control fluorophores. (a) 1 μ M FAD + 300 μ M tryptophan in the absence of magnetic fields; (b) 1 μ M fluorescein and (c) 1 μ M Alexa Fluor[®] 488 in the presence of a square wave modulated magnetic field (same conditions as in Fig. 1b). The fast decay rate for fluorescein is 2-3 times slower than that for FAD and FMN. Alexa Fluor[®] 488 is over 40 times as bright as FAD and FMN, and so fluorescence in (c) was measured at \sim 15 times lower laser power and 0.5-0.7 times the gain on the emCCD camera compared with (a), (b) and Fig. 1b-c.

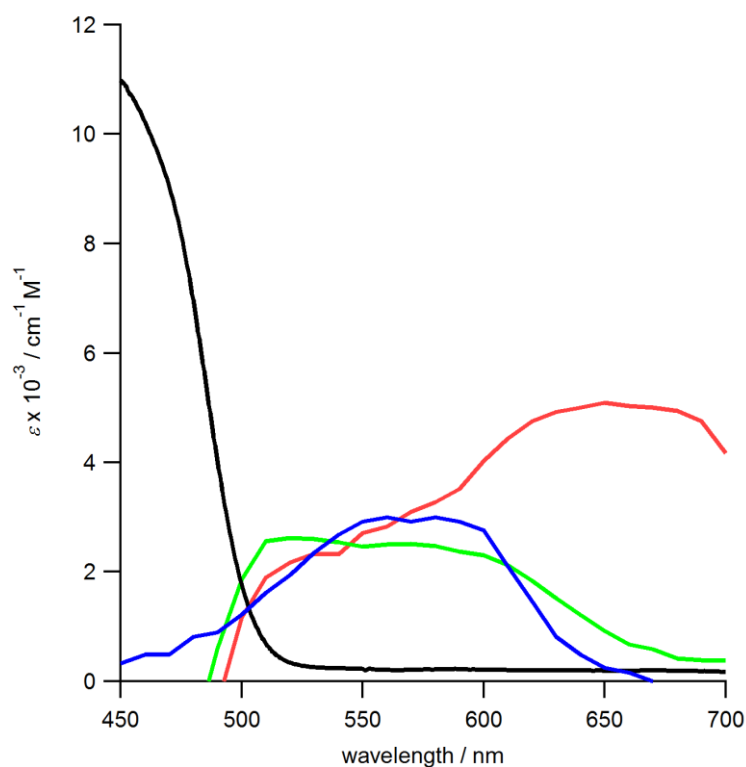


Fig. S2: Absorption spectra of flavin and tryptophan species. Absorption of FAD (black) measured at pH 2.6, absorption of flavin excited triplet state (red) and protonated flavin radical (green) taken from Ref 1, absorption of protonated Trp^{••} radical (blue) taken from Ref 2. Tryptophan itself absorbs below 300 nm.

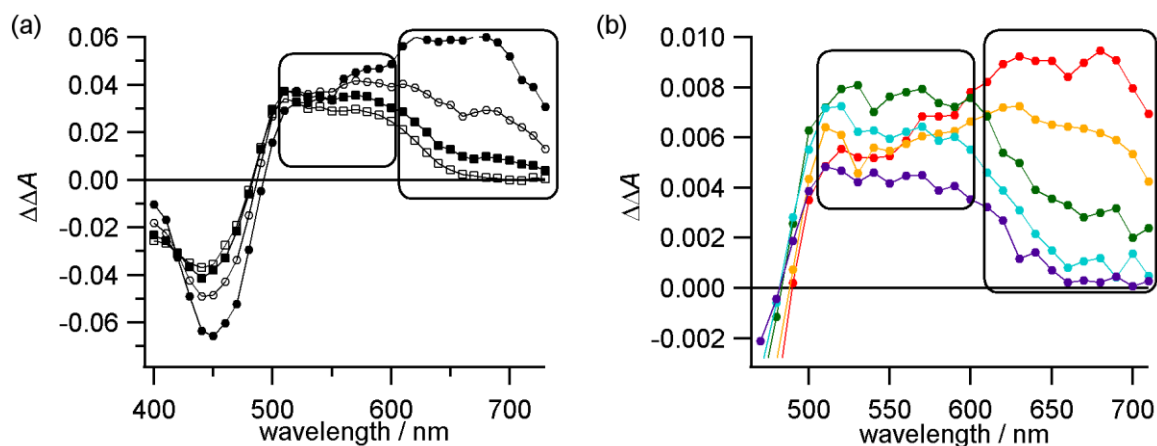


Fig. S3: Magnetic sensitivity of FAD absorption in the visible spectrum as measured by transient absorption. (a) Magnetic sensitivity over time for 0.2 mM FAD + 0.5 mM Trp. Filled circles – 0.2 μ s; open circles – 0.5 μ s; filled squares – 1.0 μ s; open squares – 5.0 μ s. (b) Magnetic sensitivity at different concentrations of Trp. Data averaged 0.5–2.0 μ s. Red – 0 mM Trp; yellow – 0.1 mM Trp; green – 0.5 mM Trp; cyan – 1.0 mM Trp; purple – 2.0 mM Trp. Boxes indicate regions of the spectrum averaged in the $\Delta\Delta A$ measurements reported in the main text.

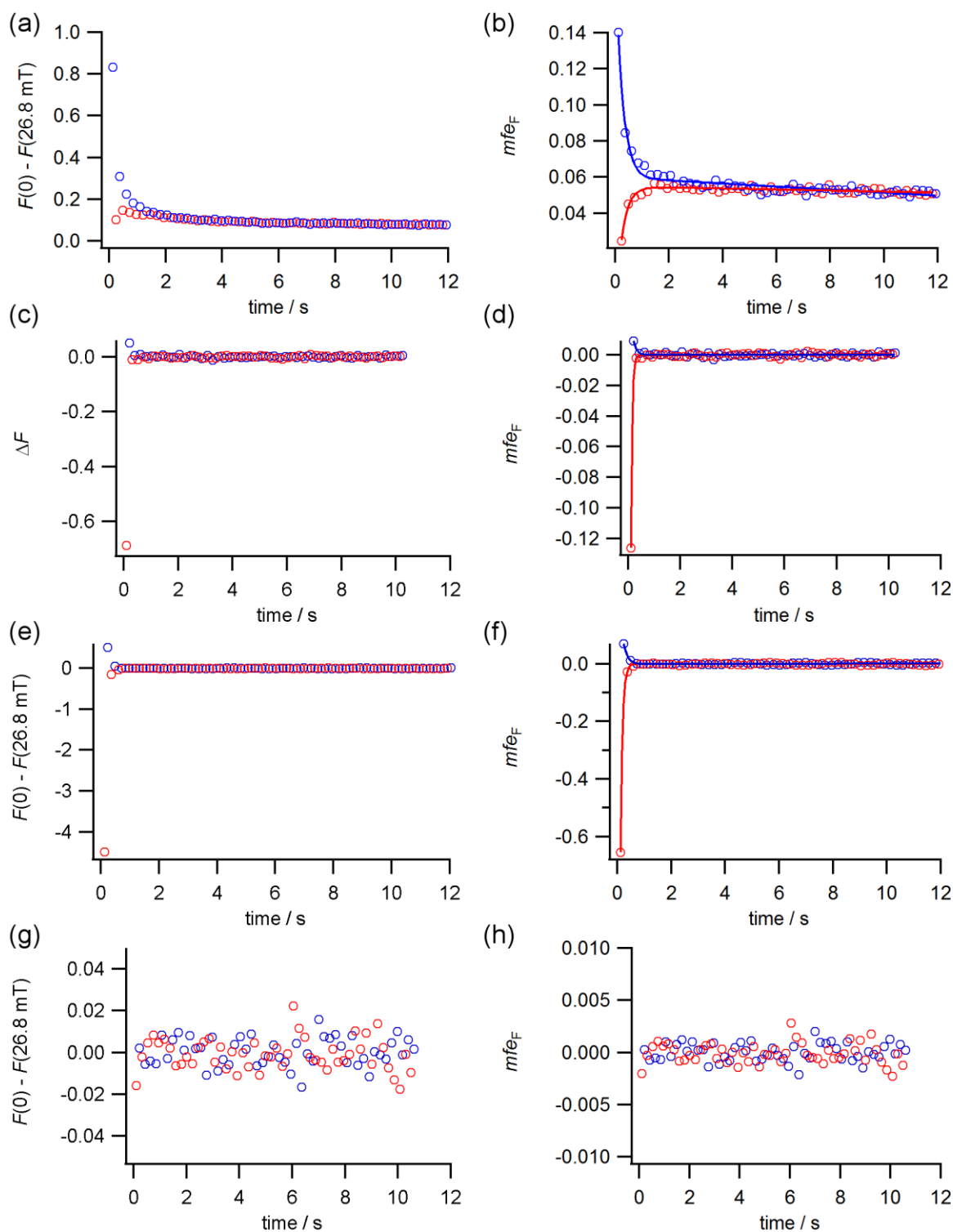


Fig. S4: Apparent time-dependence in mfe_F calculations. (a, b) 1 μ M FAD + 300 μ M Trp in the presence of a pulsed 26.8 mT magnetic field. (c, d) 1 μ M FAD + 300 μ M Trp in the absence of an applied magnetic field. Quantities calculated as 'mock' measurements using exactly the same methodology as panels (a), (b) and (e)–(h). The difference in y-axis label for panel (c) reflects the absence of magnetic fields in this 'mock' measurement. (e, f) 1 μ M FMN in the presence of a pulsed 26.8 mT magnetic field. (g, h) 1 μ M Alexa Fluor® 488 in the presence of a pulsed 26.8 mT magnetic field. Note the scale used on the Alexa measurements. Solid lines in panels (b), (d) and (f) are fits to an exponential decay plus a straight line. The extrapolation of this straight line back to the y-axis was taken to be the time-independent value of mfe_F . Blue: measurements originating in a step down (from field-off to field-on), red: measurements originating in a step up (from field-on to field-off).

REFERENCES

1. M. Murakami, K. Maeda and T. Arai, *Chem. Phys. Lett.*, 2002, **362**, 123-129.
2. S. Solar, N. Getoff, P. S. Surdhar, D. A. Armstrong and A. Singh, *J Phys. Chem.*, 1991, **95**, 3639-3643.